

Cite this: *RSC Adv.*, 2018, 8, 22046

Mixed metal $\text{Co}^{\text{II}}_{1-x}\text{Zn}^{\text{II}}_x$ –organic frameworks based on chains with mixed carboxylate and azide bridges: magnetic coupling and slow relaxation†

Yan-Qin Wang,^a Kun Wang^b and En-Qing Gao^{*b}

A series of isomorphous three-dimensional metal–organic frameworks $[\text{Co}^{\text{II}}_{1-x}\text{Zn}^{\text{II}}_x(\text{L})(\text{N}_3)] \cdot \text{H}_2\text{O}$ ($x = 0.26, 0.56$ and 0.85) based on bimetallic $\text{Co}^{\text{II}}_{1-x}\text{Zn}^{\text{II}}_x$ ($x = 0.26, 0.56$ and 0.85) chains with random metal sites have been synthesized and magnetically characterized. The $\text{Co}^{\text{II}}_{1-x}\text{Zn}^{\text{II}}_x$ series, which intrinsically feature random anisotropic/diamagnetic sites, shows complex magnetic interactions. By gradually introducing the diamagnetic Zn^{II} ions into the pure anisotropic Co^{II} single-chain magnets system, the ferromagnetic interactions between Co^{II} ions are gradually diluted. Moreover, the slow magnetic relaxation behaviour of the mixed metal $\text{Co}^{\text{II}}_{1-x}\text{Zn}^{\text{II}}_x$ systems also changes. In this bimetallic series $\text{Co}^{\text{II}}_{1-x}\text{Zn}^{\text{II}}_x$, the Co-rich materials exhibit slow relaxation processes that may arise from SCM mechanism, while the Zn^{II}-rich materials show significantly low slow magnetic relaxation. A general trend is that the activation energy and the blocking temperature decrease with the increase in diamagnetic Zn^{II} content, emphasizing the importance of anisotropy for slow relaxation of magnetization.

Received 17th April 2018

Accepted 3rd June 2018

DOI: 10.1039/c8ra03273d

rsc.li/rsc-advances

Introduction

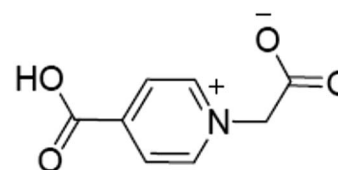
Recently, single-chain magnets (SCMs) have attracted significant attention due to their unique physical behaviours and potential applications in information storage and quantum computing between chemistry and physics.¹ Slow magnetic relaxation is characteristic for SCMs intrinsic to individual chains, which can lead to blocking of magnetization below a certain temperature. Raising the blocking temperature (T_B) is a great challenge in the study of SCMs. The general strategy is to increase the barrier of magnetic relaxation by increasing magnetic anisotropy and/or intrachain magnetic interaction. Therefore, it is of great importance for the choice of spin carriers with large magnetic anisotropy and bridging ligands between them. Although some homospin Co^{II} ,² Mn^{II} ,³ Fe^{II} and Ln^{III} ⁵ SCMs have been reported, heterospin SCMs such as mixed-valence,⁶ metal-radical,⁷ bimetallic ($3d-3d$,⁸ $3d-4d$,⁹ $3d-5d$,¹⁰ or $d-f^{\text{II}}$) and even tri-spin compounds¹² are more common because the magnetic interactions and anisotropy are easier to tune in heterospin systems.

In this context, we performed a series of systematic studies and successfully obtained several homospin SCMs. In these compounds, Co^{II} or Fe^{II} ions are bridged by simultaneous azide-carboxylate,¹³ azide-tetrazolate,¹⁴ or azide-carboxylate-tetrazolate bridges,¹⁵ and the bridges transmit ferromagnetic coupling (FO), where the formation of the particular bridging systems benefited from the use of zwitterionic pyridinium carboxylate ligands. It is worth mentioning that a family of isomorphous three-dimensional (3D) Mn^{II} , Fe^{II} , Co^{II} and Ni^{II} metal–organic frameworks (MOFs) has been obtained from different transition metal ions, azide ions and a simple zwitterionic ligand (L) (Scheme 1). The Mn^{II} MOF shows typical 1D antiferromagnetism (AF), while the anisotropic Fe^{II} , Co^{II} and Ni^{II} compounds behave as FO SCMs in 3D MOFs. Inspired by the isomorphism of these MOFs and with the aim of tuning the SCM behaviours, we focused on the magnetic behaviour of isomorphous mixed-metal systems where two different anisotropic metal ions are randomly distributed over structurally equivalent sites in variable ratios. This metal-mixing strategy has been widely used in materials science to tune the properties of materials, and the study of random mix-metal magnetic

^aCollege of Chemistry and Chemical Engineering, Inner Mongolia University, Huhhot, 010021, China. E-mail: yqwang_chem@imu.edu.cn; Fax: +86-471-4994375; Tel: +86-471-4994375

^bShanghai Key Laboratory of Green Chemistry and Chemical Processes, School of Chemistry and Molecular Engineering, East China Normal University, Shanghai 200062, P. R. China. E-mail: eqgao@chem.ecnu.edu.cn; Fax: +86-21-62233404; Tel: +86-21-62233404

† Electronic supplementary information (ESI) available. CCDC 1832808. For ESI and crystallographic data in CIF or other electronic format see DOI: 10.1039/c8ra03273d



Scheme 1 1-Carboxymethylpyridinium-4-carboxylate (HL).



materials such as metallic alloys, oxides, halides, and some rare molecular systems has revealed unusual magnetic phenomena.¹⁶ To the best of our knowledge, random bimetallic SCM systems remain largely unexplored.¹⁷ Recently, we have reported four mixed-metal systems, namely, $\text{Fe}_{1-x}\text{Mn}_x$,¹⁸ $\text{Co}_{1-x}\text{Ni}_x$,¹⁹ $\text{Fe}_{1-x}\text{Co}_x$ and $\text{Fe}_{1-x}\text{Ni}_x$.^{13a} The $\text{Fe}_{1-x}\text{Mn}_x$ system shows a gradual AF-to-FO evolution in overall behaviours as the $\text{Fe}(\text{II})$ content increases. Interestingly, we found that a Co-rich $\text{Co}_{1-x}\text{Ni}_x$ system can exhibit higher T_B than both parent materials, whereas the bimetallic $\text{Fe}_{1-x}\text{Co}_x$ system demonstrates a significantly lower T_B than both parent Fe^{II} and Co^{II} materials. Furthermore, the $\text{Fe}_{1-x}\text{Ni}_x$ materials show direct composition dependence, where the T_B decreases monotonically as Fe^{II} is replaced by the less anisotropic Ni^{II} . Herein, as a continuation of the research on mixed metal systems, we examine the $\text{Co}_{1-x}\text{Zn}_x$ series ($x = 0.26, 0.56$ and 0.85), which intrinsically features random anisotropic (Co^{II}) and diamagnetic sites (Zn^{II}), which is manifested through complex magnetic interactions. By the gradual introduction of diamagnetic Zn^{II} ions into the pure anisotropic Co^{II} single-chain magnets system, the FO interaction between Co^{II} ions is gradually diluted. Moreover, the slow magnetic relaxation behaviour is also changed. In this bimetallic series $\text{Co}^{\text{II}}_{1-x}\text{Zn}^{\text{II}}_x$, the Co-rich materials show slow relaxation behaviour that may arise in typical SCMs, and the slow magnetic relaxation is significantly reduced with the increase in diamagnetic Zn^{II} content. A general trend is that the activation energy and T_B decrease with the increase in Zn^{II} content.

Experimental section

Materials and physical measurements

The reagents were obtained from commercial sources and used without further purification. 1-Carboxymethylpyridinium-4-carboxylate (HL) was prepared according to a method reported in the literature. Elemental analyses (C, H, and N) were performed on a Perkin-Elmer 2400 CHN elemental analyzer. FT-IR spectra were recorded in the range $500\text{--}4000\text{ cm}^{-1}$ on a Nicolet NEXUS 670 spectrophotometer using KBr pellets. The X-ray diffraction (XRD) patterns were collected on a Rigaku Ultima IV X-ray diffractometer using $\text{Mo-K}\alpha$ radiation ($\lambda = 0.71073\text{ \AA}$) at 35 kV and 25 mA. Inductively coupled plasma (ICP) analysis was carried out on an IRIS Intrepid II XSP spectrometer. Magnetic measurements were performed on a Quantum Design MPMS XL5 SQUID magnetometer. The experimental susceptibilities were corrected for the diamagnetism of the constituent atoms (Pascal's tables).

Caution! Although not encountered in our experiments, azido compounds of metal ions are potentially explosive. Only a small amount of the materials should be prepared, and it should be handled with care.

$[\text{Zn}(\text{L})(\text{N}_3)] \cdot \text{H}_2\text{O}$ (**1**)

A mixture of $\text{Zn}(\text{ClO}_4)_2 \cdot 6\text{H}_2\text{O}$ (0.2 mmol, 0.075 g), HL (0.1 mmol, 0.018 g) and NaN_3 (0.40 mmol, 0.026 g) in water/ethanol (5/5 mL) was stirred for 10 min at room temperature.

Slow evaporation of the solution at room temperature yielded light orange block crystals after one day. Yield: 65% based on HL. Elem anal. calcd (%) for $\text{C}_8\text{H}_8\text{ZnN}_4\text{O}_5$: C, 32.40; H, 2.38; N, 18.89. Found: C, 32.13; H, 2.72; N, 19.36%. IR bands ($\text{KBr}, \text{cm}^{-1}$): $\nu(\text{N}_3)$ 2082 vs., $\nu(\text{COO})$ 1627s, 1563 m and 1384s.

$[\text{Co}^{\text{II}}_{1-x}\text{Zn}^{\text{II}}_x(\text{L})(\text{N}_3)] \cdot \text{H}_2\text{O}$ ($x = 0.26, 0.56$ and 0.85)

$\text{ZnNO}_3 \cdot 6\text{H}_2\text{O}$ and $\text{CoNO}_3 \cdot 6\text{H}_2\text{O}$ in ratios 13 : 37, 14 : 11 and 17 : 3 (the total quantity of the metal salts is 0.4 mmol), were dissolved in methanol (4 mL). An aqueous solution (2 mL) of HL (0.072 g, 0.40 mmol) was added, and the clear solution was heated to reflux for 10 minutes. The addition of sodium azide (0.10 g, 1.6 mmol) to the solution under stirring led to polycrystalline precipitates. After refluxing for 3 h, the solid was collected by filtration, washed with water and methanol, and dried in air. Yields: 50–85% based on metal salts. The metal ratios in the products were determined by the inductively coupled plasma (ICP) atomic emission spectrometry. The C/H/N elemental analysis results of these compounds are identical within experimental errors. The compounds exhibit almost identical IR spectra and similar PXRD patterns.

Crystal data collection and refinement

Diffraction data for **1** was collected at 293 K on a Bruker Apex II CCD area detector equipped with graphite-monochromated $\text{Mo K}\alpha$ radiation ($\lambda = 0.71073\text{ \AA}$). Empirical absorption corrections were applied using the SADABS program.²⁰ The structures were solved by the direct method and refined by the full-matrix least-squares method on F^2 using the SHELXL program, with anisotropic displacement parameters for all non-hydrogen atoms.²¹ All of the hydrogen atoms attached to carbon atoms were placed in calculated positions and refined using the riding model. The water hydrogen atoms attached to O3 were located from the difference Fourier map and refined with restrained O–H and H...H distances (3 restraints using the DFIX instruction). A summary of the crystallographic data, data collection, and refinement parameters for compound **1** is provided in Table S1,† and the selected bond lengths and angles for compound **1** are listed in Table S2.† The ccdc number for compound **1** is 1832808.

Results and discussion

Synthesis

A series of mixed-metal MOFs, $[\text{Co}_{1-x}\text{Zn}_x(\text{L})(\text{N}_3)]$, was synthesized as polycrystalline solids through the reactions of the corresponding metal salts mixed in various ratios with the zwitterionic ligand HL and NaN_3 in aqueous methanol. The compounds show almost identical IR spectra, with strong absorptions at about 2068, 1625, and 1383 cm^{-1} that are characteristic of $\nu_{\text{as}}(\text{N}_3)$, $\nu_{\text{as}}(\text{COO})$, and $\nu_{\text{s}}(\text{COO})$, respectively. The powder X-ray diffraction (PXRD) profiles are also very similar and consistent with those simulated from the single-crystal data of the Zn^{II} -only and Co^{II} -only compounds (Fig. 1), indicative of the isomorphism and phase purity across these series.



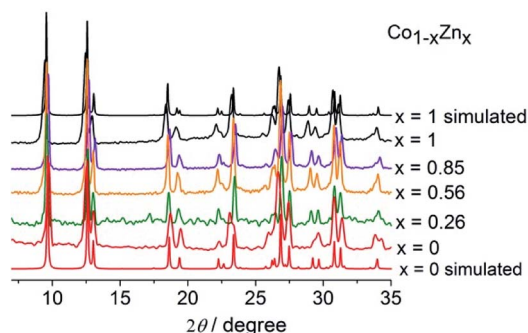


Fig. 1 PXRD patterns of the $\text{Co}_{1-x}\text{Zn}_x$ compounds.

Crystal structure

The single crystal X-ray analyses indicated that the structure of **1** was isomorphous with our previously reported compounds $[\text{Co}(\text{L})(\text{N}_3)] \cdot \text{H}_2\text{O}$ ¹⁹ and $[\text{Mn}(\text{L})(\text{N}_3)] \cdot \text{H}_2\text{O}$,¹⁸ which was a chain-based network. As shown in Fig. 2a, the unique Zn(II) assumes the centrosymmetric *trans*-octahedral $[\text{N}_2\text{O}_4]$ geometry defined by two azide nitrogen atoms (N1 and N1A) and four carboxylate oxygen atoms (O1, O1C, O2B and O2D). The Zn–O and Zn–N distances fall in the range of 2.096(2)–2.152(3) Å (Table S1,

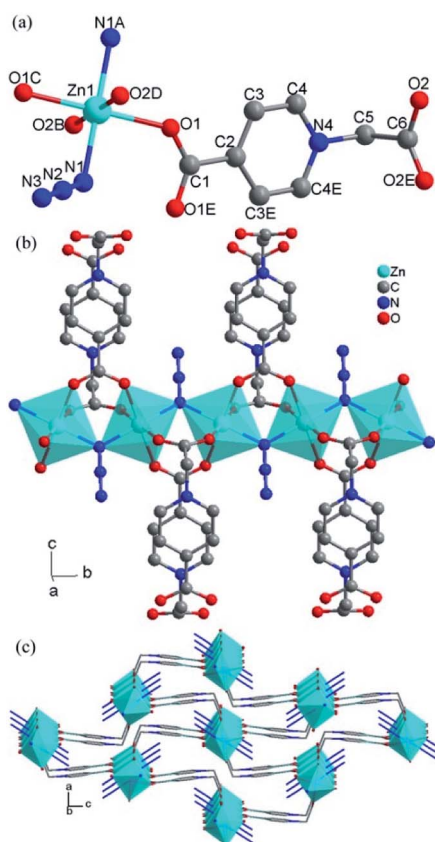


Fig. 2 (a) Local coordination environment of the Zn^{2+} center in **1** (hydrogen atoms are omitted for clarity). Symmetry code: (A) $1-x, y-0.5, 1-z$; (B) $x-0.5, y, 1.5-z$; (C) $1-x, -y, 1-z$; (D) $1.5-x, -y, z-0.5$; (E) $x, 0.5-y, z$. (b) Chain with mixed carboxylate and azide bridges. (c) 3D network.

ESI[†]). Adjacent Zn ions with $\text{Zn} \cdots \text{Zn} = 3.641(1)$ Å are bridged by an azide in the end-on mode and two carboxylate bridges in the *syn-syn* mode to yield a formally anionic chain $([\text{Zn}(\mu\text{-N}_3)(\mu\text{-OCO})_2]_n)^{n-}$ along the crystallographic *b* direction. The adjacent octahedrons along the chain share the bridging nitrogen atom with $\text{Zn-N-Zn} = 120.5(5)^\circ$ and are tilted towards each other with a dihedral angle of 54.3° between the $[\text{MO}_4]$ equatorial planes. All the bond lengths and angles are comparable with the values of isomorphous Mn(II) and Co(II) compounds.^{18,19}

Each $[\text{Zn}(\mu\text{-N}_3)(\mu\text{-OCO})_2]_n^{n-}$ chain is linked with four others by the cationic *N*-methylenepyrnidinium tethers of the L ligands to produce a neutral 3D MOF. The interchain space is divided by the L ligands bent into small channels, in which free water molecules are enclosed.

Magnetic properties of the $\text{Co}^{\text{II}}_{1-x}\text{Zn}^{\text{II}}_x$ series

The magnetic susceptibilities of the $\text{Co}_{1-x}\text{Zn}_x^{\text{II}}$ mixed-metal compounds were measured under 1000 Oe in the temperature range 2–300 K and shown as χT - T plots in Fig. 3 (top), in which, for convenience of comparison, the data for the Co^{II} ($x = 0$) parent compound is also included.

The χT values (0.56–2.71 $\text{emu mol}^{-1} \text{K}$) of the mixed-materials at 300 K are below the value of Co^{II} compound (3.30 $\text{emu mol}^{-1} \text{K}$) and decrease with Zn(II) content. For $x = 0.26$ and 0.56, the trend of χT varying with T is similar to that for **1**, showing a maximum at low temperatures. The maximum χT

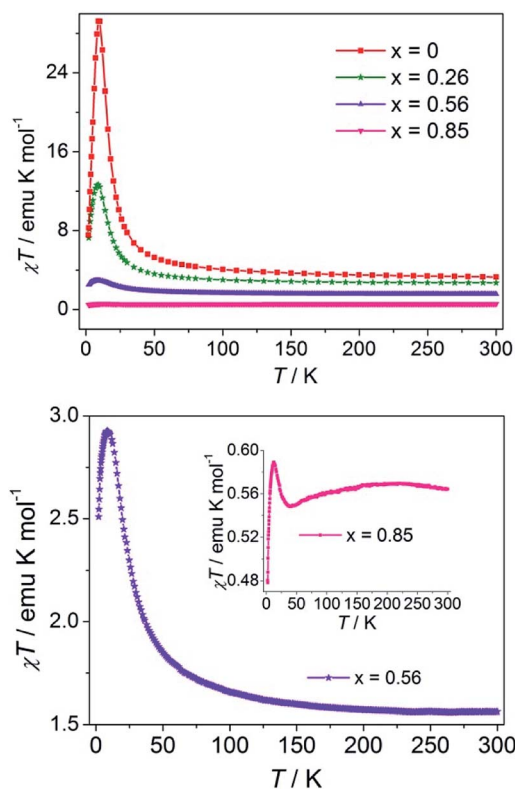


Fig. 3 Temperature dependence of χT of the $\text{Co}^{\text{II}}_{1-x}\text{Zn}^{\text{II}}_x$ series at 1000 Oe (top). The enlarged view of $\text{Co}_{1-x}\text{Zn}_x$ ($x = 0.56$ and 0.85) (bottom).



value and the corresponding temperature decrease with Zn(II) content (Fig. 3 and Table 1). The increase in χT with the decrease in temperature demonstrates FO interactions between Co(II) ions transmitted by the $(\text{OCO})_2(\text{EO-N}_3)$ triple bridges. The decrease in χT at low temperature is mainly due to the saturation effect of the relatively high applied field, a common phenomenon for ferromagnetic systems. The χ^{-1} versus T plots above 20 K for compounds with $x = 0.26$ and 30 K for compounds with $x = 0.56$ follow the Curie–Weiss law. As shown in Table 1, both the Curie constant and the Weiss temperature (Θ) decrease with the increase in Zn(II) content. The rapid decrease in Θ does not suggest weakening of the ferromagnetic coupling between Co(II) ions because the bridging moieties are the same in these compounds. Instead, the decrease in Θ is because the ferromagnetic correlation along the chain is interrupted by the diamagnetic Zn(II) ions. The trend indicates that Co(II) and Zn(II) are mixed within individual chains. If the compound was a mixture of Co(II) chains and Zn(II) chains (*i.e.*, Co(II) and Zn(II) are in separate chains), Θ would not vary with Zn(II) content (the Curie constant always decreases).

The χT - T plot of the Zn(II)-rich compound with $x = 0.85$ is slightly more complicated. Upon cooling, after a very broad maximum at around 200 K, χT decreases to a broad minimum at 40 K, then increases rapidly to a sharp maximum at 12 K, and finally drops rapidly. The complex temperature dependence is the consequence of the interplay and competition of several effects, including the magnetic interactions between Co(II) ions, the spin-orbital coupling and symmetry-distortion on single Co(II) sites, and also the field effect.²² The decrease in χT from 200 to 40 K is because the single-ion effects overcompensate the ferromagnetic interactions between Co(II) ions, and the situation is reversed at lower temperatures. The final drop should be mainly due to the field-induced saturation effect. The single-ion effects are also present in the compounds with $x = 0, 0.26$ and 0.56 , but obscured by the ferromagnetic Co(II)–Co(II) interactions. With an increase in x , increasing numbers of Co(II) ions are isolated by Zn(II) ions and finally, the ferromagnetic effect gives way to the single-ion effects.

The magnetic behaviors of the $x = 0.56$ and 0.85 compounds confirm that the metal ions are not uniformly but randomly distributed along the chain. The uniform distribution implies that Co(II) ions would be completely isolated by diamagnetic Zn(II) ions. For $x = 0.85$, two neighboring Co(II) ions would be

separated by five to six Zn(II) ions with a distance of $>21 \text{ \AA}$. The magnetic isolation would not allow for the ferromagnetic interactions observed in the compounds.

As shown in Fig. 4, the isothermal magnetization data at 2 K indicates that the larger the Co(II) content, the more rapidly the low-field magnetization increases, and the larger the magnetization at 50 kOe. There is no indication of saturation in the high-field region and the magnetization values are in the range of 0.44 – $2.07 \text{ N}\beta$ (Fig. 4, top). No appreciable hysteresis was detected for the mixed-metal compounds (Fig. 4, bottom).

The thermal ac magnetic measurements of the mixed-metal compounds ($x = 0.26$ and 0.56) at different frequencies are shown in Fig. 5. The two compounds show non-zero out-phase signals below a certain temperature, which shifts to higher temperature as the Co(II) content increases. Both χ' and χ'' data of the two compounds show frequency dependence. Nevertheless, the specific situation is different: for the compound ($x = 0.26$), χ' and χ'' data both show maxima above 2 K, while for the compound ($x = 0.56$), the χ' data shows no maxima when χ'' data shows maxima above 2 K. This phenomenon indicates that slow relaxation of magnetization occurs and the blocking temperature (T_B) increases with the increase in the FO and anisotropic components. The parameter $\phi = (\Delta T_p/T_p)/\Delta(\log f)$ (T_p is the peak temperature of χ'') has been used as a measure of the frequency dependence.²³ For compound ($x = 0.26$), $\phi = 0.14$ and for compound ($x = 0.56$), $\phi = 0.13$; both these values are in the range for superparamagnets.^{23,24} The relaxation time $\tau(T)$

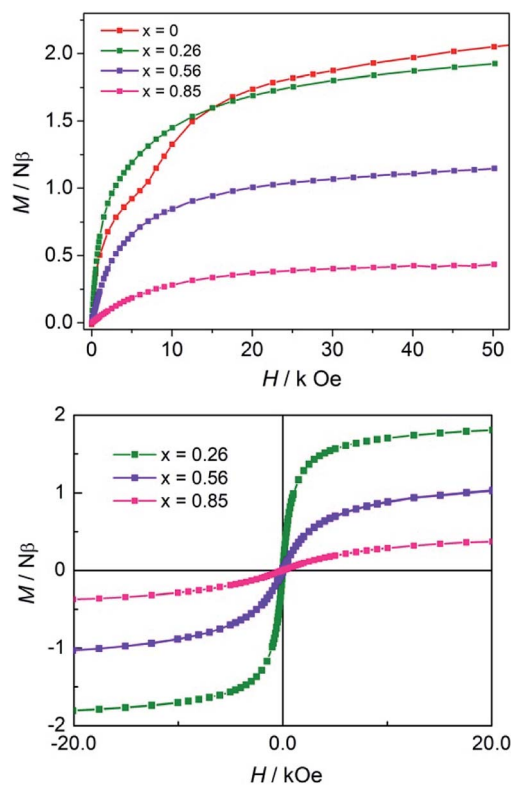


Fig. 4 Virgin magnetization curves of the $\text{Co}_{1-x}\text{Zn}_x$ compounds ($x = 0, 0.26, 0.56$ and 0.85) at 2 K (top). Hysteresis loops of compounds ($x = 0.26, 0.56$ and 0.85) at 2 K (bottom).

Table 1 Selected magnetic data for the $\text{Co}_{1-x}\text{Zn}_x$ compounds

x	0.85	0.56	0.26	0
$\chi T/\text{emu mol}^{-1} \text{ K}^a$	0.56	2.03	2.71	3.30
$T_{\text{max}}(\chi T)/\text{K}^b$	12.1	6.4	8.9	9.5
$C/\text{emu mol}^{-1} \text{ K}$	0.6	1.51	2.6	3.03
Θ/K	−0.8	8.9	13.8	27.2
Δ_c/K	—	46.1	50.5	49.7
$T_p(\chi'')/\text{K}^c$	—	3.2	3.3	3.9
M^d	0.43	1.15	1.92	2.05

^a χT value at room temperature. ^b Temperature at which χT shows a maximum at 1 kOe. ^c Temperature at which χ'' at 1 kHz shows a peak. ^d Magnetization value at 50 kOe.



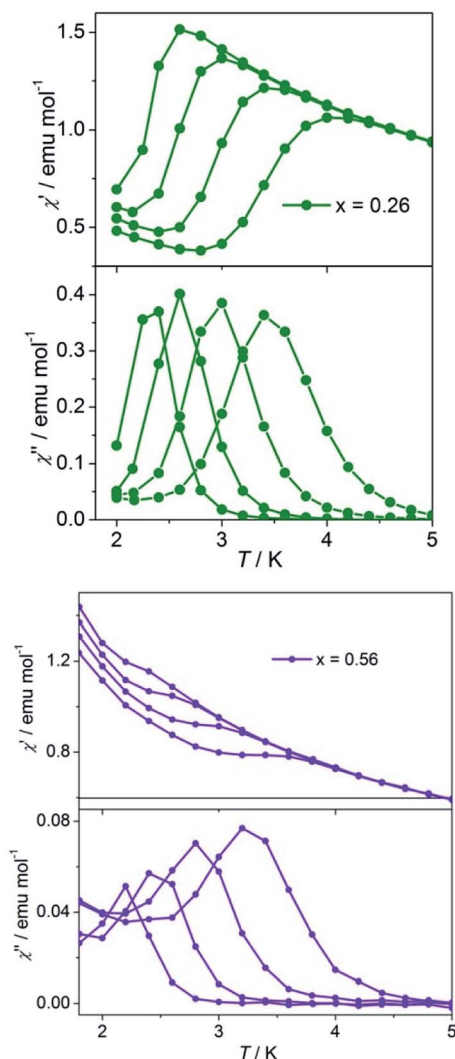


Fig. 5 AC susceptibilities of the mixed compounds at frequencies 1, 10, 100, and 1000 Hz (from left to right) with $H_{dc} = 0$ and $H_{ac} = 3.5$ Oe for compounds $x = 0.26$ (top) and $x = 0.56$ (bottom).

data obtained from the $\chi''(T)$ data of two compounds follow the Arrhenius law $\tau(T) = \tau_0 \exp(\Delta_\tau/T)$ (Fig. S1, ESI†) with $\tau_0 = 4.86 = 10^{-11}$ s and $\Delta_\tau = 50.5$ K for compound ($x = 0.26$) and $\tau_0 = 1.28 = 10^{-10}$ s and $\Delta_\tau = 46.2$ K for compound ($x = 0.56$), suggesting a thermally activated relaxation.^{18,22} The Δ_τ and τ_0 values lie in the usual range for superparamagnets including SCMs.^{1c}

Frequency dependent measurements at 2.6 K for compounds $x = 0.26$ and $x = 0.56$ were performed. For compound with $x = 0.26$ (more Co^{II} component), frequency dependent measurements produced a semicircle Cole–Cole diagram (Fig. 6), which was fitted to the generalized Debye model²⁵ with $\alpha = 0.27$, indicating a distribution of relaxation time and lies in the wide range (0.01–0.7) for reported SCMs. Compound $x = 0.56$ (less Co^{II} component) shows the dissymmetric shape of the Cole–Cole diagram (Fig. 6), which is consistent with the broad and dissymmetric $\chi''-T$ peaks and indicates the presence of additional relaxation processes and hence, cannot be fitted to the generalized Debye model. One possible origin of the additional

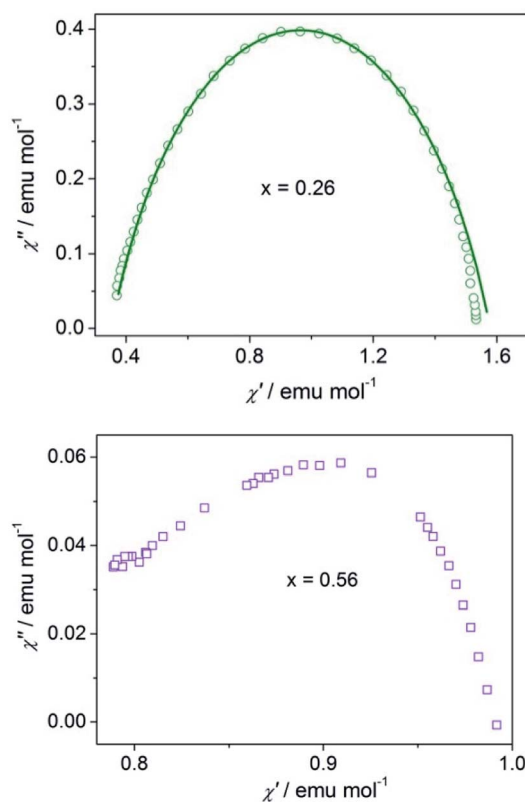


Fig. 6 Cole–Cole diagrams for the compounds with $x = 0.26$ (top) and $x = 0.56$ (bottom).

relaxation is the spin-glass dynamics, which could be associated with the inherent site randomness.

Conclusions

In conclusion, we have studied the magnetic properties of a family of isomorphous bimetallic $\text{Co}_{1-x}\text{Zn}_x$ MOFs, in which carboxylate-azide bridged chains with random $\text{Co}^{\text{II}}/\text{Zn}^{\text{II}}$ sites are interlinked by *N*-methylene pyridinium groups. It has been demonstrated that through the gradual introduction of diamagnetic Zn^{II} ions into the anisotropic Co^{II} single-chain magnets system, the FO interaction between Co^{II} ions are gradually diluted, and the slow magnetic relaxation behaviour also changes. For the bimetallic $\text{Co}^{\text{II}}_{1-x}\text{Zn}^{\text{II}}_x$ system, the Co-rich materials show slow relaxation behaviour, a mechanism related to SCMs, while the slow magnetic relaxations are significantly reduced with the increase in diamagnetic Zn^{II} content.

Conflicts of interest

There are no conflicts to declare.

Acknowledgements

We are thankful for the financial support from NSFC (21761022, 21301087, 21173083) and the Inner Mongolia autonomous region natural science fund project (2017MS0204).



Notes and references

- 1 (a) K. Liu, X. Zhang, X. Meng, W. Shi, P. Cheng and A. K. Powell, *Chem. Soc. Rev.*, 2016, **45**, 2423; (b) C. Coulon, V. Pianet, M. Urdampilleta and R. Clerac, *Struct. Bonding*, 2014, **164**, 143; (c) H. L. Sun, Z. M. Wang and S. Gao, *Coord. Chem. Rev.*, 2010, **254**, 1081; (d) W. J. Jiang, C. Q. Jiao, Y. S. Meng, L. Zhao, Q. Liu and T. Liu, *Chem. Sci.*, 2018, **9**, 617; (e) R. Li, Y. Xiao, S. H. Wang, X. M. Jiang, Y. Y. Tang, J. G. Xu, Y. Yan, F. K. Zheng and G. C. Guo, *J. Mater. Chem. C*, 2017, **5**, 513; (f) X. H. Zhao, L. D. Deng, Y. Zhou, D. Shao, D. Q. Wu, X. Q. Wei and X. Y. Wang, *Inorg. Chem.*, 2017, **56**, 8058.
- 2 (a) Y. L. Wu, F. S. Guo, G. P. Yang, L. Wang, J. C. Jin, X. Zhou, W. Y. Zhang and Y. Y. Wang, *Inorg. Chem.*, 2016, **55**, 6592; (b) X. Ma, Z. Zhang, W. Shi, L. Li, J. Zou and P. Cheng, *Chem. Commun.*, 2014, **50**, 6340; (c) M. H. Zeng, Z. Yin, Y. X. Tan, W. X. Zhang, Y. P. He and M. Kurmoo, *J. Am. Chem. Soc.*, 2014, **136**, 4680; (d) Z. S. Cai, M. Ren, S. S. Bao, N. Hoshino, T. Akutagawa and L. M. Zheng, *Inorg. Chem.*, 2014, **53**, 12546; (e) K. Chakarawet, P. C. Bunting and J. R. Long, *J. Am. Chem. Soc.*, 2018, **140**, 2058; (f) X. Y. Liu, L. Sun, H. L. Zhou, P. P. Cen, X. Y. Jin, G. Xie, S. P. Chen and Q. L. Hu, *Inorg. Chem.*, 2015, **54**, 8884; (g) G. Brunet, D. A. Safin, J. Jover, E. Ruiz and M. Murugesu, *J. Mater. Chem. C*, 2017, **5**, 835.
- 3 (a) W. X. Zhang, T. Shiga, H. Miyasaka and M. Yamashita, *J. Am. Chem. Soc.*, 2012, **134**, 6908; (b) X. Chen, S. Q. Wu, A. L. Cui and H. Z. Kou, *Chem. Commun.*, 2014, **50**, 2120; (c) Y. Z. Zhang, H. H. Zhao, E. Funck and K. R. Dunbar, *Angew. Chem., Int. Ed.*, 2015, **54**, 5583; (d) T. T. Wang, M. Ren, S. S. Bao, B. Liu, L. Pi, Z. S. Cai, Z. H. Zheng, Z. L. Xu and L. M. Zheng, *Inorg. Chem.*, 2014, **53**, 3117; (e) M. Ding, B. W. Wang, Z. M. Wang, J. L. Zhang, O. Fuhr, D. Fenske and S. Gao, *Chem.–Eur. J.*, 2012, **18**, 915.
- 4 (a) J. Boeckmann, M. Wriedt and C. Näther, *Chem.–Eur. J.*, 2012, **18**, 5284; (b) D. Shao, S. L. Zhang, X. H. Zhao and X. Y. Wang, *Chem. Commun.*, 2015, **51**, 4360; (c) Y. Z. Zheng, W. Xue, M. L. Tong, X. M. Chen, F. Grandjean and G. J. Long, *Inorg. Chem.*, 2008, **47**, 4077.
- 5 (a) E. Bartolomé, J. Bartolomé, A. Arauzo, J. Luzón, L. Badía, R. Cases, F. Luis, S. Melnic, D. Prodius, S. Shova and C. Turta, *J. Mater. Chem. C*, 2016, **4**, 5038; (b) D. T. Thielemann, M. Klinger, T. J. A. Wolf, Y. Lan, W. Wernsdorfer, M. Busse, P. W. Roesky, A. N. Unterreiner, A. K. Powell, P. C. Junk and G. B. Deacon, *Inorg. Chem.*, 2011, **50**, 11990; (c) Y. Z. Zheng, Y. Lan, W. Wernsdorfer, C. E. Anson and A. K. Powell, *Chem.–Eur. J.*, 2009, **15**, 12566.
- 6 (a) T. Liu, H. Zheng, S. Kang, Y. Shiota, S. Hayami, M. Mito, O. Sato, K. Yoshizawa, S. Kanegawa and C. Duan, *Nat. Commun.*, 2013, **4**, 2826; (b) C. Papatriantafyllopoulou, S. Zartilas, M. J. Manos, C. Pichon, R. Clerac and A. J. Tasiopoulos, *Chem. Commun.*, 2014, **50**, 14873; (c) A. Escuer, G. Vlahopoulou and F. A. Mautner, *Inorg. Chem.*, 2011, **50**, 2717.
- 7 (a) M. G. F. Vaz, R. A. A. Cassaro, H. Akpınar, J. A. Schlueter, P. M. Lahti and M. A. Novak, *Chem.–Eur. J.*, 2014, **20**, 5460; (b) T. Han, W. Shi, Z. Niu, B. Na and P. Cheng, *Chem.–Eur. J.*, 2013, **19**, 994; (c) Z. Tomkowicz, M. Rams, M. Balandá, S. Foro, H. Nojiri, Y. Krupskaya, V. Kataev, B. Buchner, S. K. Nayak, J. V. Yakhmi and W. Haase, *Inorg. Chem.*, 2012, **51**, 9983; (d) K. Bernot, L. Bogani, A. Caneschi, D. Gatteschi and R. Sessoli, *J. Am. Chem. Soc.*, 2006, **128**, 7947.
- 8 (a) N. Hoshino, F. Iijima, G. N. Newton, N. Yoshida, T. Shiga, H. Nojiri, A. Nakao, R. Kumai, Y. Murakami and H. Oshio, *Nat. Chem.*, 2012, **4**, 921; (b) L. M. Toma, C. Ruiz-Perez, J. Pasan, W. Wernsdorfer, F. Lloret and M. Julve, *J. Am. Chem. Soc.*, 2012, **134**, 15265; (c) M. Rams, E. V. Peresypkina, V. S. Mironov, W. Wernsdorfer and K. E. Vostrikova, *Inorg. Chem.*, 2014, **53**, 10291; (d) H. Miyasaka, T. Madanbashi, A. Saitoh, N. Motokawa, R. Ishikawa, M. Yamashita, S. Bahr, W. Wernsdorfer and R. Clerac, *Chem.–Eur. J.*, 2012, **18**, 3942.
- 9 (a) D. P. Zhang, L. F. Zhang, Y. T. Chen, H. L. Wang, Z. H. Ni, W. Wernsdorfer and J. Z. Jiang, *Chem. Commun.*, 2010, **46**, 3550; (b) J. F. Guo, X. T. Wang, B. W. Wang, G. C. Xu, S. Gao, L. Szeto, W. T. Wong, W. Y. Wong and T. C. Lau, *Chem.–Eur. J.*, 2010, **16**, 3524.
- 10 (a) X. Feng, J. Liu, T. D. Harris, S. Hill and J. R. Long, *J. Am. Chem. Soc.*, 2012, **134**, 7521; (b) Y. Q. Zhang, C. L. Luo, X. B. Wu, B. W. Wang and S. Gao, *Inorg. Chem.*, 2014, **53**, 3503; (c) E. V. Peresypkina, A. M. Majcher, M. Rams and K. E. Vostrikova, *Chem. Commun.*, 2014, **50**, 7150.
- 11 (a) V. Mougel, L. Chatelain, J. Hermle, R. Caciuffo, E. Colineau, F. Tuna, N. Magnani, A. de Geyer, J. Pecaut and M. Mazzanti, *Angew. Chem., Int. Ed.*, 2014, **53**, 819; (b) J. W. Zhang, X. M. Kan, B. Q. Liu, G. C. Liu, A. X. Tian and X. L. Wang, *Chem.–Eur. J.*, 2015, **21**, 16219; (c) L. Chatelain, F. Tuna, J. Pecaut and M. Mazzanti, *Chem. Commun.*, 2015, **51**, 11309.
- 12 (a) Z. X. Wang, X. Zhang, Y. Z. Zhang, M. X. Li, H. Zhao, M. Andruh and K. R. Dunbar, *Angew. Chem., Int. Ed.*, 2014, **53**, 11567; (b) M. X. Yao, Q. Zheng, K. Qian, Y. Song, S. Gao and J. L. Zuo, *Chem.–Eur. J.*, 2013, **19**, 294; (c) D. Visinescu, A. M. Madalan, M. Andruh, C. Duhayon, J. P. Sutter, L. Ungur, W. Van den Heuvel and L. F. Chibotaru, *Chem.–Eur. J.*, 2009, **15**, 11808.
- 13 (a) Y. Q. Wang, Q. Yue and E. Q. Gao, *Chem.–Eur. J.*, 2017, **23**, 896; (b) Y. Q. Wang, W. W. Sun, Z. D. Wang, Q. X. Jia, E. Q. Gao and Y. Song, *Chem. Commun.*, 2011, **47**, 6386; (c) Y. Q. Wang, X. M. Zhang, X. B. Li, B. W. Wang and E. Q. Gao, *Inorg. Chem.*, 2011, **50**, 6314; (d) J. Y. Zhang, K. Wang, X. B. Li and E. Q. Gao, *Inorg. Chem.*, 2014, **53**, 9306; (e) Q. X. Jia, H. Tian, J. Y. Zhang and E. Q. Gao, *Chem.–Eur. J.*, 2011, **17**, 1040; (f) X. M. Zhang, Y. Q. Wang, K. Wang, E. Q. Gao and C. M. Liu, *Chem. Commun.*, 2011, **47**, 1815.
- 14 X. B. Li, G. M. Zhuang, X. Wang, K. Wang and E. Q. Gao, *Chem. Commun.*, 2013, **49**, 1814.
- 15 X. B. Li, J. Y. Zhang, Y. Q. Wang, Y. Song and E. Q. Gao, *Chem.–Eur. J.*, 2011, **17**, 13883.



- 16 (a) A. N. Pirogov, J. G. Park, A. S. Ermolenko, A. V. Korolev, A. G. Kuchin, S. Lee, Y. N. Choi, J. Park, M. Ranot, J. Yi, E. G. Gerasimov, Y. A. Dorofeev, A. P. Vokhmyanin, A. A. Podlesnyak and I. P. Swainson, *Phys. Rev. B*, 2009, **79**, 174412; (b) G. C. DeFotis, G. S. Coker, J. W. Jones, C. S. Branch, H. A. King, J. S. Bergman, S. Lee and J. R. Goodey, *Phys. Rev. B*, 1998, **58**, 12178.
- 17 J. P. Zhao, B. W. Hu, X. F. Zhang, Q. A. Yang, M. S. El Fallah, J. Ribas and X. H. Bu, *Inorg. Chem.*, 2010, **49**, 11325.
- 18 Y. Q. Wang, Q. Yue, Y. Qi, K. Wang, Q. Sun and E. Q. Gao, *Inorg. Chem.*, 2013, **52**, 4259.
- 19 Y. Q. Wang, A. L. Cheng, P. P. Liu and E. Q. Gao, *Chem. Commun.*, 2013, **49**, 6995.
- 20 G. M. Sheldrick, *Program for Empirical Absorption Correction of Area Detector Data*, University of Göttingen, Germany, 1996.
- 21 G. M. Sheldrick, SHELXTL Version 5.1, *Bruker Analytical X-ray Instruments Inc.*, Madison, Wisconsin, USA, 1998.
- 22 (a) O. Kahn, *Molecular Magnetism*, Wiley-VCH, Weinheim, 1993; (b) R. L. Carlin, *Magnetochemistry*, Springer, Berlin, 1986; (c) F. Lloret, M. Julve, J. Cano, R. Ruiz-García and E. Pardo, *Inorg. Chim. Acta*, 2008, **361**, 3432.
- 23 J. A. Mydosh, *Spin Glasses: An Experimental Introduction*, Taylor & Francis, London, 1993.
- 24 (a) T. F. Liu, D. Fu, S. Gao, Y. Z. Zhang, H. L. Sun, G. Su and Y. J. Liu, *J. Am. Chem. Soc.*, 2003, **125**, 13976; (b) E. Coronado, J. R. Galán-Mascarós and C. Martí-Gastaldo, *J. Am. Chem. Soc.*, 2008, **130**, 14987.
- 25 K. S. Cole and R. H. Cole, *J. Chem. Phys.*, 1941, **9**, 341.

